Available online at www.sciencedirect.com
SCIENCE DIRECT®
Materials and Design 25 (2004) 681–688
Materials & Design
www.elsevier.com/locate/matdes

Adiabatic shear instability based mechanism for particles/substrate bonding in the cold-gas dynamic-spray process

M. Grujicic [a,*], C.L. Zhao [a], W.S. DeRosset [b], D. Helfritch [b]

[a] *Program in Materials Science and Engineering, Department of Mechanical Engineering, 241 Engineering Innovation Building, Clemson University, Clemson, SC 29634-0921, USA*

[b] *Army Research Laboratory – Processing and Properties Branch, Aberdeen, Proving Ground, MD 21005-5069, USA*

Received 11 September 2003; accepted 4 March 2004
Available online 7 June 2004

Abstract

Particles/substrate interactions during the cold-gas dynamic-spray deposition process are studied using a dynamic axisymmetric thermo-mechanical finite element analysis. In addition, the particles/substrate bonding mechanism has been investigated using a one-dimensional thermo-mechanical model for adiabatic strain softening and the accompanying adiabatic shear localization. The results obtained show that the minimal impact particles velocity needed to produce shear localization at the particles/substrate interface correlates quite well with the critical velocity for particles deposition by the cold-gas dynamic-spray process in a number of metallic materials. This finding suggests that the onset of adiabatic shear instability in the particles/substrate interfacial region plays an important role in promoting particle/substrate adhesion and, thus, particles/substrate bonding during the cold-gas dynamic-spray process.

Keywords: Cold-gas dynamic-spray; Adiabatic shear localization

1. Introduction

The cold-gas dynamic-spray process, often referred to as ''cold spray'', is a high-rate coating and free-form fabrication process in which fine, solid powder particles (generally 1–50 μm in diameter) are accelerated to velocities in a range between 500 and 1000 m/s by entrainment in a supersonic jet of compressed (propellant) gas. The solid particles are directed toward a substrate, where upon impact, they undergo plastic deformation and bond to the surface, rapidly building up a layer of the depositing material. Cold spray as a coating technology was initially developed in the mid-1980s at the Institute for Theoretical and Applied Mechanics of the Siberian Division of the Russian Academy of Science in Novosibirsk [1,2]. The Russian scientists successfully deposited a wide range of pure metals, metallic alloys, polymers and composites onto a variety of substrate materials. In addition, they demonstrated that very high coating deposition rates on the order of 3 m^2/min (~300 ft^2/min) are attainable using the cold-spray process.

A simple schematic of a typical cold-spray device is shown in Fig. 1. Compressed gas of an inlet pressure on the order of 30 bar (500 psi) enters the device and flows through a converging/diverging DeLaval-type nozzle to attain a supersonic velocity. The solid powder particles are metered into the gas flow upstream of the converging section of the nozzle and are accelerated by the rapidly expanding gas. To achieve higher gas flow velocities in the nozzle, the compressed gas is often preheated. However, while preheat temperatures as high as 900 K are sometimes used, due to the fact that the contact time of spray particles with the hot gas is quite short and that the gas rapidly cools as it expands in the diverging section of the nozzle, the temperature of the particles remains substantially below the initial gas preheat temperature and, hence, below the melting temperature of the powder material.

Because of its low-temperature operation, the cold-spray process generally offers a number of advantages

* Corresponding author. Tel.: +864-656-5639; fax: +864-656-4435.
E-mail address: mica.grujicic@ces.clemson.edu (M. Grujicic).

0261-3069/$ - see front matter © 2004 Elsevier Ltd. All rights reserved.
doi:10.1016/j.matdes.2004.03.008

Report Documentation Page

Form Approved
OMB No. 0704-0188

1. REPORT DATE	2. REPORT TYPE	3. DATES COVERED
2004		**00-00-2004 to 00-00-2004**

4. TITLE AND SUBTITLE	5a. CONTRACT NUMBER
Adiabatic shear instability based mechanism for particles/substrate bonding in the cold-gas dynamic-spray process	5b. GRANT NUMBER
	5c. PROGRAM ELEMENT NUMBER
6. AUTHOR(S)	5d. PROJECT NUMBER
	5e. TASK NUMBER
	5f. WORK UNIT NUMBER
7. PERFORMING ORGANIZATION NAME(S) AND ADDRESS(ES) **Celmson University,Department of Mechanical Engineering,Clemson,SC,29634**	8. PERFORMING ORGANIZATION REPORT NUMBER
9. SPONSORING/MONITORING AGENCY NAME(S) AND ADDRESS(ES)	10. SPONSOR/MONITOR'S ACRONYM(S)
	11. SPONSOR/MONITOR'S REPORT NUMBER(S)

12. DISTRIBUTION/AVAILABILITY STATEMENT
Approved for public release; distribution unlimited

13. SUPPLEMENTARY NOTES

14. ABSTRACT

Particles/substrate interactions during the cold-gas dynamic-spray deposition process are studied using a dynamic axisymmetric thermo-mechanical finite element analysis. In addition, the particles/substrate bonding mechanism has been investigated using a one-dimensional thermo-mechanical model for adiabatic strain softening and the accompanying adiabatic shear localization. The results obtained show that the minimal impact particles velocity needed to produce shear localization at the particles/substrate interface correlates quite well with the critical velocity for particles deposition by the cold-gas dynamic-spray process in a number of metallic materials. This finding suggests that the onset of adiabatic shear instability in the particles/substrate interfacial region plays an important role in promoting particle/substrate adhesion and, thus, particles/substrate bonding during the cold-gas dynamic-spray process.

15. SUBJECT TERMS

16. SECURITY CLASSIFICATION OF:			17. LIMITATION OF ABSTRACT	18. NUMBER OF PAGES	19a. NAME OF RESPONSIBLE PERSON
a. REPORT	b. ABSTRACT	c. THIS PAGE			
unclassified	**unclassified**	**unclassified**	**Same as Report (SAR)**	**8**	

Nomenclature

C_p	specific heat
D_{th}	thermal diffusivity
T	temperature
t	time
v	velocity
x	characteristic system dimension
t	time
ε^p	equivalent normal plastic strain
σ^e	equivalent normal flow stress
ρ	density

Subscripts

c	particles/substrate contact quantity
init	initial quantity
Melt	melt-temperature quantity
p	particle quantity

Superscripts

e	equivalent-normal quantity
p	plastic-deformation quantity

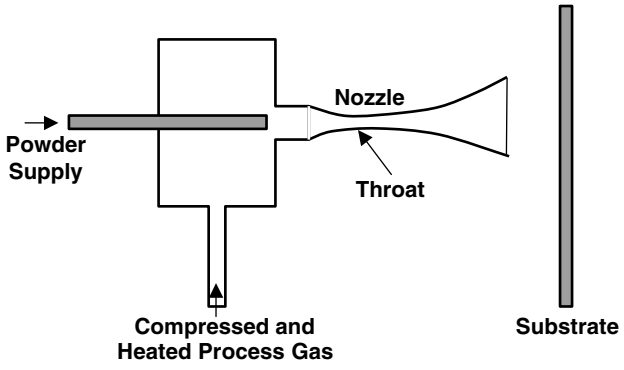

Fig. 1. Schematic of a typical cold-spray system.

over the thermal-spray material deposition technologies, such as oxy-fuel, detonation gun, plasma, arc sprays, and others. Among these advantages, the most important appear to be: (a) the amount of heat delivered to the coated part is relatively small so that microstructural changes in the substrate material are minimal or non-existent; (b) due to the absence of in-flight oxidation and other chemical reactions, thermally and oxygen-sensitive depositing materials (e.g. copper or titanium) can be cold sprayed without significant material degradation; (c) nanophase, intermetallic and amorphous materials, which are not amenable to conventional thermal spray processes (due to a major degradation of the depositing material), can be cold sprayed; (d) formation of the embrittling phases is generally avoided; (e) macro- and micro-segregations of the alloying elements during solidification which accompany the conventional thermal-spray techniques and can considerably compromise materials properties do not occur during cold spraying. Consequently, attractive properties of the powder material are retained in cold-sprayed bulk materials; (f) "peening" effect of the impinging solid particles can give rise to potentially beneficial compressive residual stresses in cold-spray deposited materials [3] in contrast to the highly detrimental tensile residual stresses induced by solidification shrinkage accompanying the conventional thermal-spray processes; and (g) cold spray of the materials like copper, solder and polymeric coatings offers exciting new possibilities for cost-effective and environmentally friendly alternatives to the technologies such as electroplating, soldering and painting [4].

The actual mechanism by which the solid particles deform and bond during cold spray is still not well understood. It is well established, however, that the feed-powder particles and the substrate/deposited material undergo an extensive localized deformation during impact. This causes disruption of the thin (oxide) surface films and enables an intimate conformal contact between the particles and the substrate/deposited material. The intimate conformal contact of clean surfaces combined with high contact pressures are believed to be necessary conditions for particles/substrate and particles/deposited material bonding. This hypothesis is supported by a number of experimental findings such as: (a) a wide range of ductile (metallic and polymeric) materials can be successfully cold-sprayed while non-ductile materials such as ceramics can be deposited only if they are co-cold-sprayed with a ductile (matrix) material; (b) the mean deposition particle velocity should exceed a minimum (material-dependent) critical velocity to achieve deposition which suggests that sufficient kinetic energy must be available to plastically deform the solid material and/or disrupt the surface film; and (c) the particle kinetic energy at impact is typically significantly lower than the energy required to melt the particle suggesting that particle/substrate and particle/deposited material bonding is primarily, or perhaps entirely, a solid-state process. The lack of melting is directly confirmed through micrographic examination of the cold-sprayed materials [2].

In a recent work, Assadi et al. [5] carried out a comprehensive experimental and computational finite element analysis of the copper cold-spraying deposition process. The results of Assadi et al. [5] suggest that cold-spray bonding mechanism can be attributed to adiabatic shear instability which occurs at the particle/substrate or particle/deposited material interfaces at high impact

particle velocities. In the present paper, the analysis of Assadi et al. [5] is extended to several other metallic material systems and a more detailed analysis of the susceptibility of metallic materials to adiabatic shear instability during cold spray is investigated.

The organization of the paper is as follows: A brief overview of the finite element procedure used to simulate the cold-spray deposition process is presented in Section 2. An analysis of the adiabatic shear instability is discussed in Section 3. The main results obtained in the present work are presented and discussed in Section 4. The key conclusions resulting from the present study are summarized in Section 5.

2. Finite element computational analysis

The interaction of a single particle with the substrate upon impact is analyzed using a dynamic finite element analysis and the commercial finite element program ABAQUS/Explicit, Version 6.3 [6]. The particle is assumed to impact the substrate in a direction normal to the substrate surface. This assumption makes the problem at hand axisymmetric, eliminating the need for a computationally intensive three-dimensional analysis. Following Assadi et al. [5], the particle/substrate interaction is assumed to be an adiabatic process, that is, the heat transfer is not considered. The validity of this assumption can be assessed by comparing the thermal diffusion distance, $\sqrt{D_{\mathrm{th}}t_{\mathrm{c}}}$ (D_{th} is the thermal diffusivity, t_{c} is the particle/substrate "contact" time during which a non-zero pressure acts on the particle/substrate interface) with, x, the characteristic system dimension (the average edge length of a finite element). For the typical values $D_{\mathrm{th}} = 10^{-6}$ m^2/s and $t_{\mathrm{c}} = 10^{-8}$ s, the thermal diffusion distance, $\sqrt{D_{\mathrm{th}}t_{\mathrm{c}}}$, takes on a valueof about 1.7×10^{-6} m. Since this value is relatively small in comparison with the average finite element edge length, $x \approx 0.3 \times 10^{-6}$ m, the neglect of heat conduction during the particle/substrate collision appears justified. Assadi et al. [5] further showed that the adiabatic assumption made is justified even if, due to small system dimensions, heat transfer is assumed to be controlled by the lattice waves (the phonons).

A schematic of the (axisymmetric) computational domain involving a spherical particle and a cylindrical substrate, along with the initial and the boundary conditions used are given in Fig. 2. Both the particle and the substrate are modeled as strain-hardening, strain-rate sensitive and thermal-softening materials in which the equivalent normal plastic deformation resistance, σ^{e}, is given by the Johnson–Cook plasticity model [7] as

$$\sigma^{\mathrm{e}} = [A + B(\varepsilon^{\mathrm{p}})^n][1 + C\ln(\dot{\varepsilon}^{\mathrm{p}}/\dot{\varepsilon}_0^{\mathrm{p}})][1 - (\frac{T - T_{\mathrm{init}}}{T_{\mathrm{melt}} - T_{\mathrm{init}}})^m] \quad (1)$$

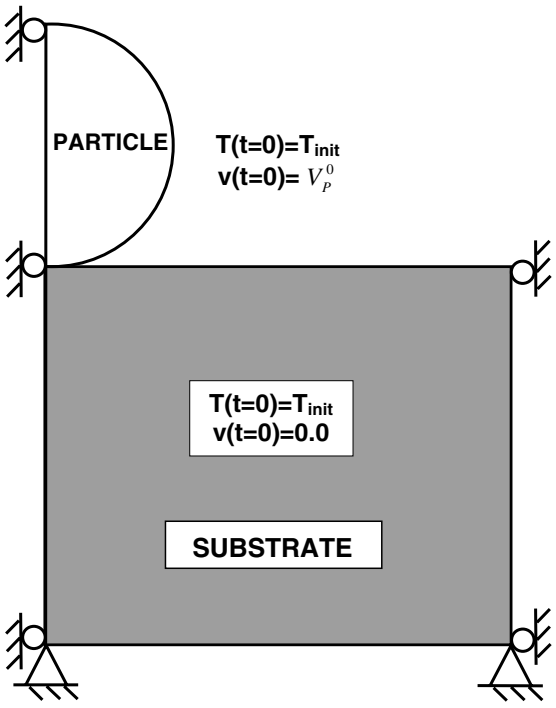

Fig. 2. An axisymmetric computational domain and the initial and the boundary conditions of the particle/substrate interaction during the cold-spray deposition process.

where ε^{p} is the equivalent normal plastic strain, $\dot{\varepsilon}^{\mathrm{p}}$ the equivalent normal plastic strain rate, $\dot{\varepsilon}_0^{\mathrm{p}}$ a reference equivalent normal plastic strain rate, T the temperature, and the subscripts init and melt are used to denote the initial and the melting temperatures, respectively. The Johnson–Cook plasticity model parameters: A, B, n, C, m and T_{melt} are taken from the CTH database [8]. The remaining details of the finite element analysis carried out in the present work such as, optimization of the mesh size and its effect on convergence can be found in [9].

3. Analysis of shear instability and localization

The phenomenon of adiabatic shear instability and the associated formation of shear bands was first considered in sufficient details by Wright [10,11]. To understand this phenomenon on a simple physical level, typical dynamic stress–strain curves (obtained during experiments such as the thin-walled tube-torsion Kolsky bar experiment) are shown in Fig. 3(a). For a typical work-hardening material under non-adiabatic conditions, the stress–strain curve (denoted as "*Isothermal* " in Fig. 3(a)) shows a monotonic increase of the flow stress with plastic strain. However, under adiabatic conditions, the plastic strain energy dissipated as heat increases the temperature causing material softening. Consequently, the rate of strain hardening decreases and

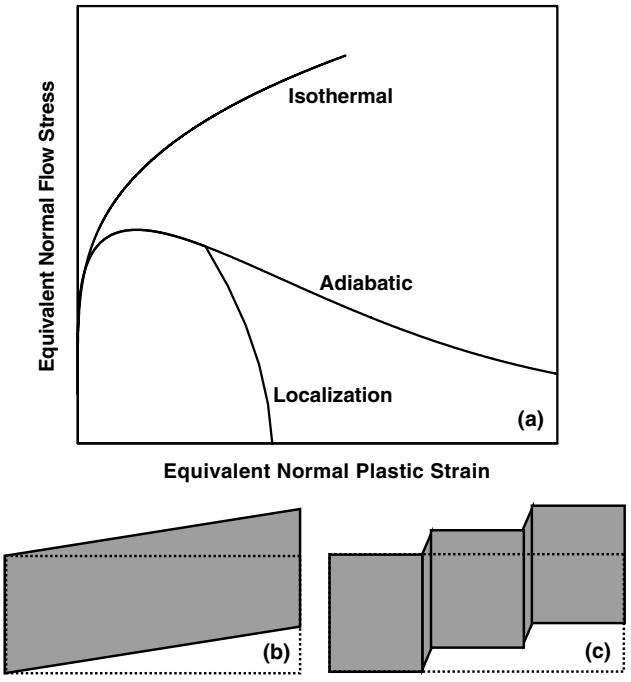

Fig. 3. (a) Schematics of the stress–strain curves in a normal strain-hardening material ("Isothermal"), an adiabatically softened material ("Adiabatic") and in a material undergoing an adiabatic shear localization ("Localization"); (b) and (c) schematics of the uniform and the localized simple shears, respectively. Initial material elements are denoted using dotted lines while sheared elements are denoted using solid lines in (b) and (c).

the flow stress reaches a maximum value, past which a monotonic decreases in the flow stress with plastic strain takes place (the curve labeled "*Adiabatic*" in Fig. 3(a)). In an ideal material with uniform distributions of stress, strain, temperature and materials microstructure, softening can continue indefinitely. In real materials, however, fluctuations in stress, strain, temperature or microstructure, and the inherent instability of strain softening can give rise to plastic flow (shear) localization. Under such circumstances, shearing and heating (and consequently softening) become highly localized, while the straining and heating in the surrounding material regions practically stops. This, in turn, causes the flow stress to quickly drop to zero (the curve denoted "*Localization*" in Fig. 3(a)). Simple schematics are used in Figs. 3(b) and (c) to demonstrate the basic difference between the uniform (simple) shear and the localized (simple) shear.

To analyze the onset of strain softening and adiabatic shear localization, a simple one-dimensional model is developed in the present work. The model is used to reveal the thermo-mechanical behavior of a small material element at the particle/substrate interface during the particle/substrate collision. The model consists of the following governing equations and initial conditions:

The *equivalent plastic strain rate*, $\dot{\varepsilon}^{\mathrm{p}}$:

$$\dot{\varepsilon}^{\mathrm{p}} = \dot{\varepsilon}^{\mathrm{p}}_{\mathrm{c}} \frac{\rho v_{\mathrm{p}}^2}{2} \cdot \frac{1}{\sigma^{\mathrm{e}}}, \quad \dot{\varepsilon}^{\mathrm{p}}(t=0) = \dot{\varepsilon}^{\mathrm{p}}_{\mathrm{c}} \frac{\rho (v_{\mathrm{p}}^0)^2}{2} \cdot \frac{1}{A}. \tag{2}$$

The *equivalent plastic strain*, ε^{p}:

$$\varepsilon^{\mathrm{p}} = \int_0^t \dot{\varepsilon}^{\mathrm{p}} \, \mathrm{d}t, \quad \varepsilon^{\mathrm{p}}(t=0) = 0. \tag{3}$$

The *heating rate*, $\dot{T}$:

$$\dot{T} = \frac{\sigma^{\mathrm{e}} \dot{\varepsilon}^{\mathrm{p}}}{\rho C_{\mathrm{p}}}, \quad \dot{T}(t=0) = \frac{A \dot{\varepsilon}^{\mathrm{p}}(t=0)}{\rho C_{\mathrm{p}}}. \tag{4}$$

The *temperature*, T:

$$T = \int_0^t \dot{T} \, \mathrm{d}t, \quad T(t=0) = T_{\mathrm{init}}. \tag{5}$$

The *particle velocity*, v_{p}:

$$v_{\mathrm{p}} = v_{\mathrm{p}}^0 \left(1 - \frac{t}{t_{\mathrm{c}}}\right), \quad v_{\mathrm{p}}(t=0) = v_{\mathrm{p}}^0. \tag{6}$$

The *equivalent plastic flow strength*, σ^{e}:

$$\sigma^{\mathrm{e}} = [A + B(\varepsilon^{\mathrm{p}})^n][1 + C \ln(\dot{\varepsilon}^{\mathrm{p}}/\dot{\varepsilon}^{\mathrm{p}}_0)] \times \left[1 - \left(\frac{T - T_{\mathrm{init}}}{T_{\mathrm{melt}} - T_{\mathrm{init}}}\right)^m\right], \quad \sigma^{\mathrm{e}}(t=0) = A, \tag{7}$$

where $\dot{\varepsilon}^{\mathrm{p}}_0$ is a strain rate proportionally constant, ρ the (constant) material mass density, C_{p}, the (constant) specific heat and a raised dot is used to denote the time derivative of a quantity.

In the model presented above the following assumptions are made:

(a) The particle velocity is assumed to decrease linearly with time from its initial value v_{p}^0 to a zero value at $t = t_{\mathrm{c}}$.
(b) The contact pressure at the particle/substrate or particle/deposited material interface in assumed to be proportional to the kinetic energy of the particle per unit volume, $\rho v_{\mathrm{p}}^2/2$.
(c) The particle deformation energy is taken to be completely dissipated in the form of heat, i.e. the energy of deformation stored in the form of various deformation-induced microstructural defects is assumed to be negligibly small.
(d) Variations of the materials properties such as ρ and C_{p} with plastic strain, stress or temperature are ignored.

The model described above enables determination of time evolutions of the plastic strain rate, plastic strain, heating rate, temperature and the equivalent stress in a typical material element at the particle/substrate interface during a particle/substrate collision. The model is solved using a simple forward difference method. As will be shown in Section 3, this procedure clearly demonstrates a transition of the stress–strain curve from a strain-hardening type to a strain-softening type at high impact particle velocities.

To analyze the tendency of a strain-softening material to undergo strain (shear) localization, the approach of Schoenfeld and Wright [12] is utilized. According to Schoenfeld and Wright [12], the tendency for strain localization measured by the inverse of the amount of uniform plastic strain taking place past the strain at which the flow stress experiences a maximum needed to obtain strain localization scales with the *SL* parameter defined as:

$$SL = \left(-\frac{\partial^2 \sigma^e / (\partial \varepsilon^p \partial \varepsilon^p)}{(\partial \sigma^e / \partial \dot{\varepsilon}^p)\sigma^e} \right)_{\sigma^e = \sigma^e_{max}}, \quad (8)$$

where σ^e_{max} denotes the maximum value of the (adiabatic) flow stress at a given impact particle velocity. A numerical solution of the model presented above enables evaluation of the *SL* parameter and, hence, quantification of the relative tendency of different materials for shear localization.

4. Results and discussion

4.1. Results of the finite element analysis

The finite element analysis of the cold-spray deposition process carried out in the present work has encompassed the following combinations of the material and process parameters:

(a) particle diameter: 5 μm and 25 μm;
(b) initial particle velocity: 400–800 m/s in 50 m/s increments;
(c) particle and substrate materials: copper, aluminum, nickel, 316L stainless steel and Ti–6Al–4V. All possible same-material combinations of the particle and the substrate materials and selected dissimilar-material particle/substrate combinations are considered.

A typical time evolution of the particle and the substrate shapes during impact of a particle onto the substrate is shown in Figs. 4(a)–(d). The results displaced in Figs. 4(a)–(d) pertain to the case of a copper particle with a 25-μm diameter and the initial impact velocity of 550 m/s colliding with a flat copper substrate at a right angle relative to the substrate surface. Both the particle and the substrate are initially at room temperature (295 K). The results displayed in Figs. 4(a)–(d), as well as the respective results obtained for different combinations of the material and process parameters can be briefly summarized as following:

(a) As the particle penetrates the substrate, a crater is being developed in the substrate.
(b) The diameter and the depth of the crater increase as the particle/substrate contact time increases while the height-to-width aspect ratio of the particle decreases.
(c) The plastic deformation in the particle and in the substrate is concentrated in a narrow region surrounding the particle/substrate interface and,

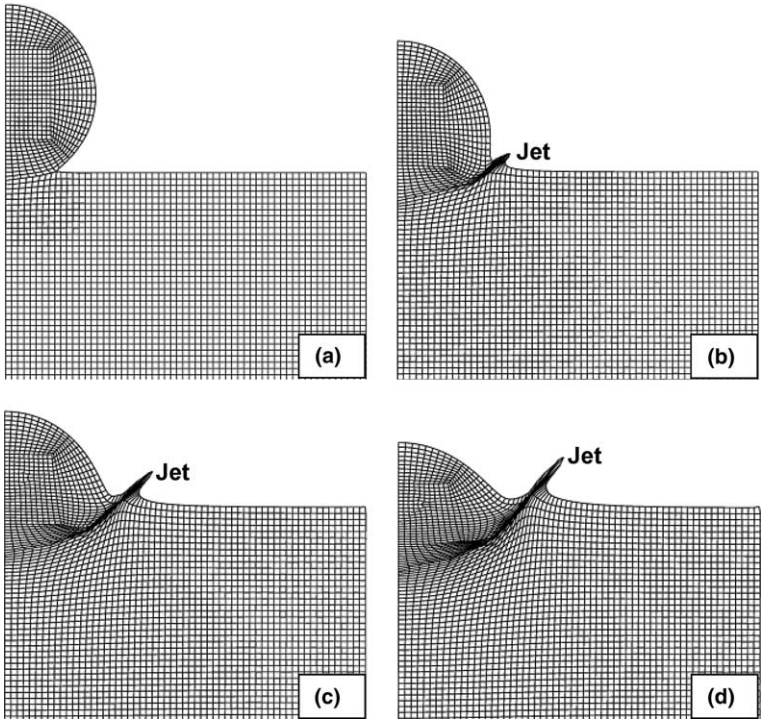

Fig. 4. Temporal evolution of the particle and the substrate materials during the particle collision with the substrate. Particle/substrate contact time: (a) 4.4 ns; (b) 13.2 ns; (c) 22.0 ns and (d) 30.8 ns.

consequently, an interfacial jet composed of the highly deformed material is formed.

(d) Due to localization of the plastic deformation to a region surrounding the particle/substrate interface, a significant temperature increase is observed only in this region (the results not shown for brevity).

(e) As the impact particle velocity increases, for a given combination of the particle and substrate materials, the thickness of the interfacial jet decreases indicating an increased level of plastic strain localization in the interfacial region.

(f) At a given impact particle velocity and for a given combination of the particle and the substrate materials, the effect of the particle diameter (in the 5–25 μm range) on the evolution of the particle and the substrate shapes during impact is not significant.

(g) For a given impact particle velocity, and when the particle and the substrate are composed of different materials, inversion of the particle and the substrate materials, generally, has a significant effect on the crater diameter and the crater depth, as well as on the thickness of the interfacial jet. In general, when the particle material possesses a larger density, the crater diameter and the depth are larger. In addition, the thickness of the interfacial jet is larger when the particle material is stiffer and less dense. The last observation suggests that as the sound velocity (scales with a ratio of the elastic modulus and the density) in the particle material increases, the extent of the plastic strain localization decreases.

To reveal the tendency for the development of adiabatic shear localization in the particle/substrate interfacial region, the temporal evolution of the equivalent plastic strain rate, the equivalent plastic strain, the temperature and the equivalent normal stress are monitored in several elements at the lower surface of the particle and at the upper surface of the substrate. An example of the typical results obtained is given in Figs. 5(a)–(d). The results displayed in Fig. 5(a)–(d) pertain to the case of a copper particle with a 25-μm diameter and a copper substrate. The results displayed in Figs. 5(a)–(d) can be summarized as following:

(a) At lower impact particle velocities ($v_p = 400$–550 (m/s), temporal evolutions of the equivalent normal plastic strain rate, the equivalent normal plastic strain, the temperature and the equivalent normal stress show a monotonic change with the particle/substrate contact time.

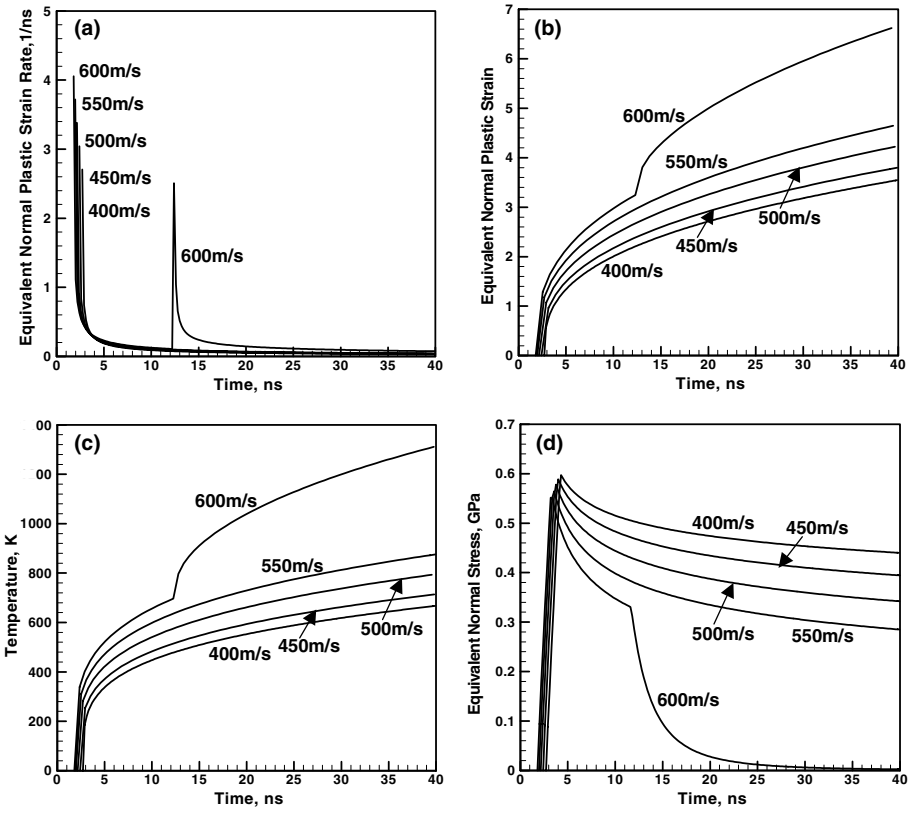

Fig. 5. Temporal evolutions of: (a) the equivalent plastic strain rate; (b) the equivalent plastic strain; (c) the temperature; and (d) the equivalent normal stress in an element at the copper-particle surface during the particle collision with a copper substrate for various initial impact particle velocities.

Table 1
A comparison of the threshold impact particle velocities obtained in the present work with the corresponding velocities reported by Assadi et al. [5]

Particle material	Substrate material	Threshold particle velocity (m/s)		
		Assadi et al. [5]	Present work – finite element analysis	Present work – shear localization analysis
Copper	Copper	570–580	575–585	571
Aluminum	Aluminum	760–770	760–770	766
Nickel	Nickel	600–610	620–630	634
316L	316L	600–610	620–630	617
Titanium	Titanium	670–680c	650–670	657
Copper	Aluminum	N/A	510–530	507
Aluminum	Copper	N/A	600–630	634
Copper	Nickel	N/A	570–580	571
Nickel	Copper	N/A	570–580	576
Copper	316L	N/A	570–580	574
316L	Copper	N/A	570–580	573
Copper	Titanium	N/A	520–550	514
Titanium	Copper	N/A	570–590	582

(b) At the highest particle velocities used ($v_p = 600$ m/s, in the case of Figs. 5(a)–(d)), temporal evolutions of the equivalent plastic strain rate, the equivalent plastic strain, the temperature and the equivalent normal stress are monotonic to a certain particle/substrate contact time. Past this contact time, the equivalent plastic strain rate, the equivalent plastic strain, the temperature undergo an abrupt increase, while the equivalent normal stress undergoes an precipitous decrease to a value near zero.

These findings are fully consistent with the temporal evolution of a material element which undergoes adiabatic softening culminating in adiabatic shear localization (curve denoted "Localization" in Fig. 3(a)). A comparison between the minimal impact particle velocity needed to produce shear localization in the particle/substrate interfacial region (obtained using the present finite element analysis) and the threshold velocity for cold-spray deposition reported by Assadi et al. [5] is given in Table 1. It is seen that in general there is a good correlation between the two sets of values for a number of materials suggesting that shear localization indeed plays a critical role in the cold-spray deposition process.

4.2. One-dimensional adiabatic shear localization analysis

In this section, the one-dimensional model for adiabatic shear localization developed in Section 3 is used to predict the minimal impact particle velocity needed to give rise to adiabatic shear localization in the particle/substrate interfacial region. Based on the results of the finite element analysis presented in Section 4.1, it is established that localization in a material element at the particle or substrate surface occurs when the shear localization parameter, SL, takes on a value larger than about $1.6 \times 10^{-4} \pm 0.2 \times 10^{-4}$ s/GPa. This finding is somewhat surprising since it suggests that all materials and material combinations have comparable tendencies for strain localization past the point of maximum flow strength. Assuming that $SL = 1.6 \times 10^{-4}$ s/GPa can be considered as a critical condition for the onset of adiabatic shear localization, the one-dimensional model presented in Section 3 is used to determine the minimum value of the particle velocity required to achieve this critical value of SL. This was done by using a simple computational procedure within which the initial particle velocity is varied in the increments of 10 m/s, and the value of SL evaluated at the peak level of the equivalent normal stress using Eq. (8). The results obtained are listed in the last column in Table 1. These results are found to be a very weak function of the model parameters, $\dot{\varepsilon}_c^p$ and t_c. A comparison of these results with their finite element counterparts and with the results reported by Assadi et al. [5] shows that the agreement between the three sets of results is quite reasonable. This finding suggests that the simple one-dimensional model for the onset of adiabatic shear localization can be used to assess the critical (minimal) impact particle velocity required for successful cold-spray deposition. Once such velocity is determined, an iso-entropic fluid dynamics model such as the ones developed by Dykhuizen and Smith [13] and by Grujicic et al. [14] can be used to identify the corresponding cold-gas dynamic-spray parameters (the propellant gas, the gas temperature and pressure, etc.) needed to obtain the desired average particle velocity.

4.3. The role of adiabatic softening and shear localization in cold-spray bonding

The results presented in Sections 4.1 and 4.2 suggest that adiabatic softening and adiabatic shear localization play an important role in particle/substrate bonding during the cold-spray deposition process. This conclusion

was also reached by Assadi et al. [5], but the actual mechanism by which adiabatic softening and adiabatic shear localization promote bonding was not provided. In this section an attempt is made to provide a more detailed picture of the interplay between adiabatic softening and adiabatic shear localization on one hand and particle/substrate bonding on the other.

Due to very short particle/substrate contact times, atomic diffusion is not expected to play a significant role in particle/substrate bonding. This can be readily proven as follows: The metal-metal inter-diffusion coefficient at temperatures near the melting point is of the order of 10^{-15}–10^{-13} m^2/s, and for a typical particle/substrate contact time of 40 ns, the atomic inter-diffusion distance is between 0.004 and 0.1 nm. Since this distance is only a fraction of the inter-atomic distance, atomic diffusion at the particle/substrate interface should be excluded as a dominant particle/substrate bonding mechanisms under the dynamic cold-spray deposition conditions.

Adhesion is a nano-length scale phenomenon involving atomic interactions between the contacting surfaces. Adhesion does not generally involve atomic diffusion but requires clean surfaces and relatively high contact pressures to make the surfaces mutually conforming. Adiabatic shear localization and the associated formation of the interfacial jets during cold spraying can be expected to produce clean contacting surfaces. In addition, adiabatic softening of the material in the particle/substrate interfacial region combined with relatively high contact pressures promote formation of mutually conforming contacting surfaces via plastic deformation of the contacting surfaces. Hence, once the conditions for the onset of adiabatic shear localization (and adiabatic softening) are attained at sufficiently high impact particle velocities, the conditions for extensive adhesion of the particle and substrate surfaces are reached resulting in particle/substrate bonding. In other words, adiabatic softening and adiabatic shear localization enhanced adhesion appears to be the dominant cold-spray particle/substrate bonding mechanism.

5. Conclusions

Based on the results obtained in the present work, the following main conclusions can be drawn:

1. A dynamic finite element analysis can be used to study the interactions between the feed-powder particles and the substrate during the cold-gas dynamic-spray process.
2. Such an analysis carried out in the present work reveals that the plastic deformation localizes to a thin region adjacent to the particle/substrate interface.
3. Localization of the plastic strain to the interfacial region combined with the thermal-softening effects leads to adiabatic shear instability in this region. This causes the injection of an interfacial jet consisting of the highly deformed material. The interfacial jet removes the oxide films from the surfaces of the particle and the substrate enabling an intimate contact of clean metallic surfaces and hence promoting particle/substrate bonding.

Acknowledgements

The material presented in this paper is based on work supported by the US Army Grant Number DAAD19-01-1-0661. The authors are indebted to Drs. Walter Roy and Fred Stenton of the ARL for the support and a continuing interest in the present work. The authors also acknowledge the support of the Office of High Performance Computing Facilities at Clemson University.

References

[1] Alkhimov AP, Papyrin AN, Dosarev VF, Nestorovich NI, Shuspanov MM. Gas dynamic spraying method for applying a coating. US Patent 5,302,414, 12th April; 1994.
[2] Tokarev AO. Structure of aluminum powder coatings prepared by cold gas dynamic spraying. Met Sci Heat Treat 1996;35(2):136–9.
[3] McCune RC, Papyrin AN, Hall JN, Riggs WL, Zajchowski PH. An exploration of the cold gas-dynamic spray method for several material systems. In: Berndt CC, Sampath S, editors. Thermal spray science and technology. ASM International; 1995. p. 1–5.
[4] Bishop CV, Loar GW. Practical pollution abatement method for metal finishing. Plat Surf Finish 1993;80(2):37–9.
[5] Assadi H, Gärtner F, Stoltenhoff T, Kreye H. Bonding mechanism in cold gas spraying. Acta Mater 2003;51(3):4379–94.
[6] ABAQUS/Explicit 6.3 User Manual. Pawtucket, RI: Hibbitt, Karlsson & Soerensen; 2003.
[7] Johnson GR, Cook WH. A constitutive model and data for metals subjected to large strains, high strain rates, and high temperatures. In: Proceedings of Seventh International Symposium on Ballistics. The Netherlands: The Hague; 1983. p. 541–7.
[8] Hertel ES, Bell RL, Elrick MG, Farnsworth AV, Kerley GI, McGlaun JM, et al. CTH: a software family for multi-dimensional shock physics analysis. Presentation at 19th International Symposium on Shock Waves, Marseille, France, July 26–30; 1993.
[9] Grujicic M, Saylor JR, Beasley DE, DeRosset WS, Helfritch D. Computational analysis of the interfacial bonding between feed powder particles and the substrate in the cold-gas dynamic-spray process. Appl Surf Sci 2003;219(1):211–327.
[10] Wright TW. Shear band susceptibility: work hardening materials. Int J Plasticity 1992;8(2):583–602.
[11] Wright TW. Toward a defect invariant basis for susceptibility to adiabatic shear bands. Mech Mater 1994;17(1):215–22.
[12] Schoenfeld SE, Wright TW. A failure criterion based on material instability. Int J Solids Struct 2003;40(4):3021–37.
[13] Dykhuizen RC, Smith MF. Gas dynamic principles of cold spray. J Therm Spray Technol 1998;7(3):205–12.
[14] Grujicic M, DeRosset WS, Helfritch D. Flow analysis and nozzle-shape optimization for the cold-gas dynamic-spray process. J Eng Manuf 2003;217(1):1–11.